

Three-dimensional subsurface modeling of mineralization: a case study from the Handeresi (Çanakkale, NW Turkey) Pb-Zn-Cu deposit

Sinan AKISKA^{1*}, İbrahim Sönmez SAYILI², Gökhan DEMİRELA³

¹Department of Geological Engineering, Faculty of Engineering, Ankara University, Tandoğan, Ankara, Turkey

²Fe-Ni Mining Company, Balgat, Ankara, Turkey

³Department of Geological Engineering, Faculty of Engineering, Aksaray University, Aksaray, Turkey

Received: 05.06.2012 • Accepted: 19.12.2012 • Published Online: 13.06.2013 • Printed: 12.07.2013

Abstract: The main goal of 3D modeling studies in the mining sector is to address the complex geological, mineralogical, and structural factors in subsurface environments and detect the ore zone(s). In order to solve this complexity, use of quality data (e.g., a wide range of boreholes at regular intervals) is necessary. However, this situation is not always possible because of certain restrictions such as intensive vegetation, high slope areas, and some economic constraints. At the same time, with the development of computer technology, the unused and/or insufficiently considered data need to be gathered and reviewed. This assessment may lead to the detection of potential new zone(s) and/or could prevent unnecessary costs. In this study, the target area that was chosen had inadequate and unusable data, and we used the data as effectively as possible. The Handeresi area is located in the Biga Peninsula of northwestern Turkey. In this area, the Pb-Zn-Cu occurrences take place in carbonate levels of metamorphic rocks or at the fractures and cracks of other metamorphic rocks. The area is being explored actively now. In this study, using the borehole data, we attempted to model the subsurface of this area in 3D using commercial RockWorks2006® software. As a result, there were 3 ore zones that were seen intensively in this area. One of them indicates the area in which the adits are now operating. The others could be new potential zones.

Key words: NW Anatolia, Biga Peninsula, inverse distance weighting, kriging, lead, zinc, copper, interpolation method

1. Introduction

Three-dimensional (3D) interpretation of subsurface characteristics has been used in the mining sector for a long time. Before the use of state-of-the-art computer software, portrayal of the 3D features was done using two-dimensional (2D) specialized maps, cross-sections, and fence diagrams. Currently, it is possible to construct 3D subsurface models easily using 3D Geoscientific Information Systems (3D GIS), which have efficient data-management capabilities (Rahman 2007). In the last 2 decades, the number of 3D subsurface modeling studies has increased due to the use of computer software (e.g., Renard & Courrioux 1994; de Kemp 2000; Xue *et al.* 2004; Feltrin *et al.* 2009; Ming *et al.* 2010; Akiska *et al.* 2010b). High-definition 3D models are constructed using the interpolation algorithms of those software programs; in addition, the determination of underground mines and their conditions of formation can be obtained. Because of connections between the study areas and the data that have some differences in all 3 dimensions, 3D GIS is important (Rahman 2007). The application areas of 3D GIS are: determining ore and oil deposits (e.g., Houlding

1992; Sims 1992; Feltrin *et al.* 2009; Wang *et al.* 2011), hydrogeological studies (e.g., Turner 1992; Houlding 1994), various civil engineering projects (e.g., Özmutlu & Hack 1998; Veldkamp *et al.* 2001; Elkadi & Huisman 2002; Rengers *et al.* 2002; Özmutlu & Hack 2003; Zhu *et al.* 2003; Hack *et al.* 2006; Bistacchi *et al.* 2008), modeling structural factors (Renard & Courrioux 1994; de Kemp 2000; Galera *et al.* 2003; Zanchi *et al.* 2009), and establishing settlement areas (e.g., Rahman 2007). The main aim of 3D modeling of ore deposits is to determine the complex geological, structural, and mineralogical conditions in these areas and to detect the location of these deposits in the subsurface environment. With the help of recent 3D subsurface modeling studies, some information can be gained not only about detecting ore locations but also about the formation conditions of the deposits (e.g., Feltrin *et al.* 2009).

Optimizing the subsurface data collected from various sources (boreholes, geophysical methods, well logs, etc.) could minimize the costs of many operations. Because of the complex spatial relationship existing in the subsurface environment, regularly spaced boreholes and good-quality data are necessary to resolve this complexity (Hack *et*

* Correspondence: akiska@eng.ankara.edu.tr

al. 2006). However, this situation is not always possible due to economic constraints and the difficulties of field conditions.

In Turkey, some institutions such as the General Directorate of Mineral Research and Exploration of Turkey (MTA), Turkish Petroleum Corporation (TPAO), General Directorate of State Hydraulic Works (DSİ), and others have thousands of meters of borehole log data. These data were interpreted using old technology, and much of the information is no longer used today. In fact, some of these data were taken casually and could not be associated with the subsurface characteristics (especially due to the technological deficiencies at that time) and/or could not be interpreted due to inadequacies in the number of boreholes in the study areas. With the development of new technology, these unused data need to be gathered and reviewed. New ore zones can then be detected, and unnecessary costs can be prevented by means of the reviewed data.

The goals of this study were to determine the potential Pb-Zn ore zones in the subsurface environment of the Handeresi Cu-Pb-Zn deposit by means of the surface and borehole geologic data, and to provide focus on mining

operations in specific areas in spite of obstacles such as insufficient borehole units, structural factors, and intensive vegetation. In addition, it is hoped that this study will make a contribution to more detailed modeling studies.

2. Geological setting

The study area is located in the Biga Peninsula of northwestern Turkey. It is situated between the Edremit (Balıkesir) and Yenice (Çanakkale) districts, and lies to the south of Kazdağ Massif in the western section of the Sakarya Zone (Figure 1). This zone is represented by Pre-Jurassic basement rocks that are deformed, and it includes metamorphosed and unmetamorphosed Jurassic-Tertiary units. The area consists of Devonian (Okay *et al.* 1996) granodiorite rocks called Çamlık granodiorite, a Permo-Triassic (Okay *et al.* 1990) metamorphic sequence called the Karakaya Complex, and Oligo-Miocene (Krushensky 1976) granitoid and volcanic rocks. The common rocks in the metamorphic sequence are sericite-graphite schists, phyllites, and quartzites with metasandstone and marble lenses (Figure 2). The Pre-Jurassic clues of the basement units are strongly overprinted by Alpidic deformations (Okay *et al.* 2006).

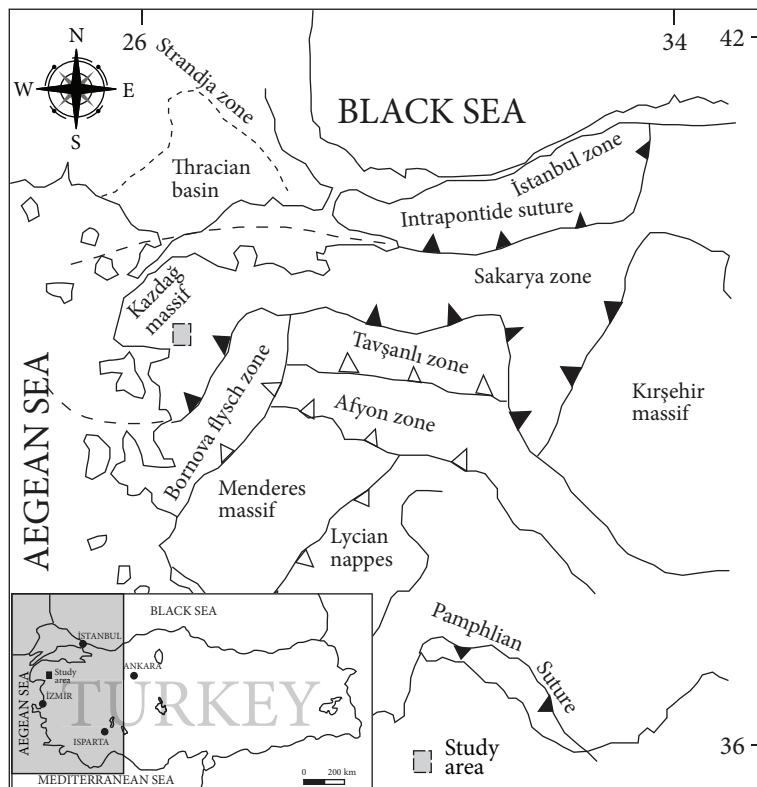


Figure 1. Simplified tectonic map showing the location of the main Tethyan sutures and neighboring tectonic units in western Turkey (after Okay *et al.* 1990; Harris *et al.* 1994).

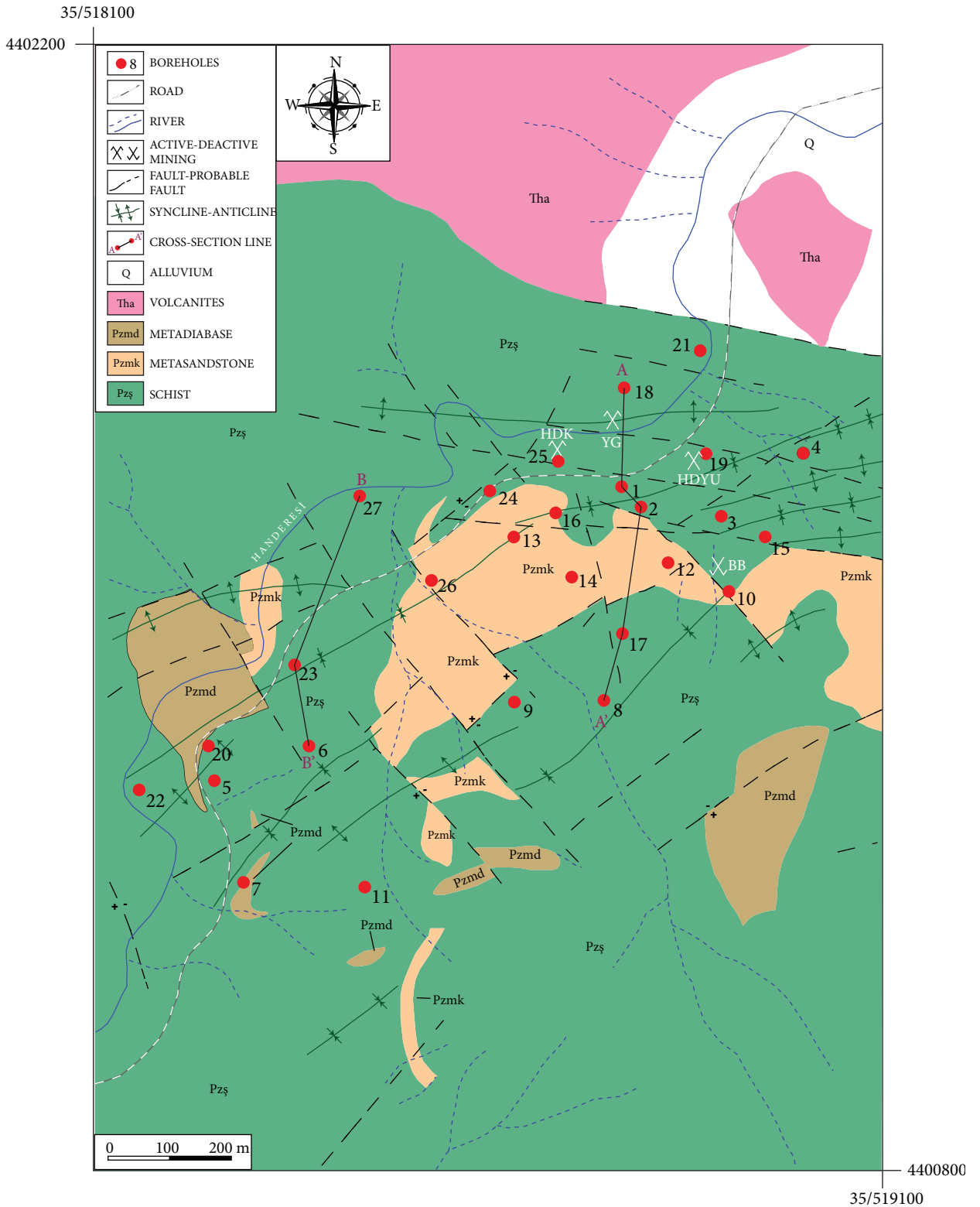


Figure 2. Geologic map of the Handeresi area including the cross-section lines between the boreholes; coordinates are given in UTM coordinate system (modified from Yücelay 1976).

Some vein- and skarn-type lead, zinc, and copper deposits are located in the Permo-Triassic metamorphic sequence (Yücelay 1976; Çağatay 1980; Çetinkaya *et al.* 1983; Tufan 1993; Akıska 2010). Mineralized zones occur in carbonate levels of metamorphic rocks or at the fractures and cracks of other metamorphic rocks. The main ore mineral paragenesis is galena, sphalerite, chalcopyrite, pyrite, arsenopyrite, and hematite assemblage, while gangue minerals are grossularitic and andraditic garnets, manganiferous hedenbergitic pyroxenes, epidote, quartz, and calcite (Akıska 2010; Akıska *et al.* 2010a; Demirela *et al.* 2010).

When the Handeresi Pb-Zn-Cu deposit was explored in the early 1970s by the MTA, 27 boreholes were drilled for mineral exploration. The Handeresi deposit is one of the most important Pb-Zn-Cu occurrences in Turkey, with total mineral resources of 3.5 Mt at an average grade of 7% Pb, 4% Zn, and 3000 g/t Cu (Yücelay 1976). In this area, mining activities have been maintained for about 40 years. The deposit is currently mined by Oreks Co. Ltd., which has produced ores from 4 adits in this area.

3. Methods

As pointed out previously, subsurface modeling studies are quite important in mining sectors, and detailed modeling studies can be achieved as a result of developments in computer technology. Particularly, assigning adit directions accurately in an underground mining area can reduce the various operating costs associated with mining.

Several software programs that are used for surface and subsurface modeling include several spatial interpolation algorithms such as nearest neighbors, inverse distance weighting (IDW), kriging, and triangulated irregular network-related interpolations (Li & Heap 2008). Each software program has its own advantages and disadvantages, but all of them have almost every one of the interpolation algorithms used in modeling studies (Rahman 2007). In this study, modeling was accomplished with commercial RockWorks2006® software, which enables the use and capability of the interpretation in conjunction with all of the data in much less time. This program includes 2 main windows: *Borehole Manager* and *Geologic Utilities*. *Borehole Manager* contains the borehole procedures such as entry, management, and analysis of borehole data. *Geologic Utilities* has mapping, gridding, and contouring properties (Rahman 2007). In this study, *Borehole Manager* is used for subsurface modeling and *Geologic Utilities* is used for surface modeling (Figure 3).

In this study, the database is created using borehole, topographic, and geologic data, and a digital elevation model (DEM) is generated via topographic data. DEM is used especially in GIS applications constructing 3D surface modeling. A 3D topographic map is generated by determining the unknown points from certain points through various interpolation methods. That is why choosing the right interpolation method is very important for creating DEMs. Many researchers have revealed the relationship between DEM accuracy and the interpolation

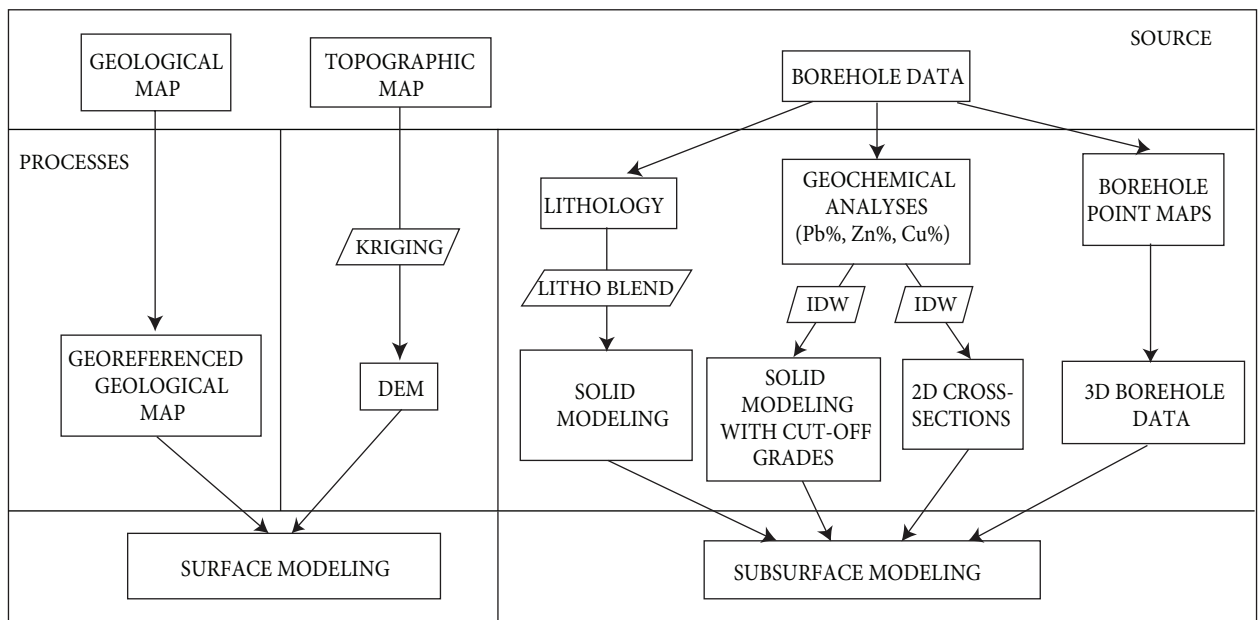


Figure 3. Organigram of the modeling processes (modified from Kaufmann & Martin 2008) (the words in the parallelograms indicate the interpolation methods).

technique (Zimmerman *et al.* 1999; Binh & Thuy 2008; and references therein). Fencik and Vajsáblová (2006) investigated the accuracy of the DEM using the kriging interpolation technique with different variogram models in the Morda-Harmonia area. As a result of this study, the authors concluded that the most appropriate variogram was a linear model. Chaplot *et al.* (2006) created DEMs using various interpolation techniques (kriging, IDW, multiquadratic radial basis function, and spline) in regions of France and Laos. The authors concluded that all interpolation techniques showed similar performance in the regions with dense sample points, while IDW and kriging were better than the others in regions with low density sample points. However, the study carried out by Peralvo (2004) in 2 watersheds of the Eastern Andean Cordillera of Ecuador showed a different result. According to this study, the IDW interpolation method produced the most incorrect DEM. In the evaluation of these studies referred to by Binh and Thuy (2008), the authors noted that the studies showed contradictory results due to the differences in technological application levels, research methods, and the types of topography in different countries. In their study, Binh and Thuy (2008) created DEMs via 3 interpolation techniques in 4 different areas in Vietnam using digital photogrammetry and total station/GPS research methods. As a result, regularized spline interpolation is the most suitable algorithm in mountainous regions, while IDW or an ordinary kriging interpolation algorithm with the exponential variogram model is recommended in hilly and flat regions (Binh & Thuy 2008). When all the data are evaluated together, even though some points are important while choosing the interpolation method that creates the DEM, there are no specific rules for choosing the interpolation algorithms. Nevertheless, considering the work done by Binh and Thuy (2008), because the area in this study includes flat and hilly areas, the kriging interpolation method is preferred for surface modeling.

Kriging (Krige 1951; introduced by Matheron 1960) is the generic name of generalized least-squares regression algorithms (Li & Heap 2008). This method is a well-known geostatistical interpolation method that weights the surrounding measured values to derive a prediction for an unmeasured location (Cressie 1990). This algorithm is an estimation process that determines the unknown values using the known values and variograms. Kriging is considered the most reliable method for geological and mining applications (Rahman 2007). The most important advantage of kriging, compared with other estimation methods, is that the weights are determined via certain mathematical operations instead of randomly. The data are analyzed systematically and objectively; as a result of this analysis, weights that will be used in variogram functions

are calculated (Tercan & Saraç 1998). Another advantage of this method is that it gives the error estimation via the kriging variance. The kriging variance does not depend on the exact values of the data; it is a function between the numbers of data and the distances of data (Tercan 1996). Very close estimation of data generated by the kriging interpolation algorithms to the real values depends on the number of samples, the frequency of data, and the degree of accuracy of the variogram model and parameters (Brooker 1986; Chaouai & Fytas 1991). The method creates variogram models of the data set that represent the relation of the variance of the data pairs with distance. This variogram indicates the extent of the spatial autocorrelations and the variogram models that could be isotropic or anisotropic, depending on the directional variability of the data. The unknown values are predicted based on the variogram model (Cressie 1990). Most frequently used in several variogram models are spherical, exponential, linear, and Gaussian models (Burrough & McDonnell 1998).

While doing subsurface modeling, RockWorks2006 performs solid modeling. Solid modeling is a grid process in 3 dimensions, which creates a cube from regularly spaced nodes derived from irregularly spaced data. During 3D modeling, the subsurface is divided into cells that have specific dimensions called voxels, and the geologic units that correspond to these cells form the cubes. Each voxel created is identified by the corner points, called nodes. Each node has an x, y, and z location coordinate, and a g value, which in this study is a geochemical analysis value. In this study, 2 different solid models are made. The first model is applied to "ORE ZONE", shown in the boreholes. The second model is applied to Pb%, Zn%, and Cu% values obtained from these ore zones.

In the first model, RockWorks2006 uses a solid modeling algorithm that is designed specifically to interpolate lithologies in the boreholes. Using this algorithm, which is called "*litho blend*", the subsurface is separated into block diagrams and all lithologies are modeled (RockWare 2006). In this study, all lithologic units are modeled; however, only "ORE ZONE" is used for the purpose of the study.

In the second model, in order to model the percentage distribution of ore zones in the boreholes, Pb%, Zn%, and Cu% values are modeled with 3D solid modeling. In this modeling study, to generate the block diagrams in the subsurface, the IDW interpolation method is preferred, which makes a distinction with respect to the similarity of degrees of the measured points. In other words, in the estimation of the unknown points, it gives more weight to the closest known points instead of the remote ones. IDW is very versatile and an easily understandable programmable method. In addition, it gives very accurate

results in wide-range data interpretation (Lam 1983). The most important feature of this method is that it is able to quickly interpolate the scattered data in the regular grids or the irregularly spaced data (Li & Heap 2008).

4. Geostatistical analysis of the surface data

The number of x, y coordinates and z elevation data points in the area is 5292. These data are digitized from the topographic map from Yücelay (1976). The topographic map has a 10-m contour interval of the study area. The information about the survey method was not given by Yücelay (1976).

As mentioned above, the modeling studies are carried out using RockWorks2006 commercial software. However, for the geostatistical analysis, more comprehensive software is needed. Therefore, the geostatistical analysis is done with the Geostatistical Analyst Tool in ArcGis9® (Johnston *et al.* 2001).

The changes depending on the distance of the difference between regionalized variable values are revealed with the variogram function in geostatistics (Tercan 1996). When the variogram is calculated in different ways, it sometimes exhibits different behaviors (Armstrong 1998). Anisotropy is used for calculating the directional effects in the semivariogram model, which is made for surface calculations. It is characteristic of a random process that indicates higher autocorrelation in one direction than another (Johnston *et al.* 2001). In this study, the surface data indicate anisotropy. The range values are different while the sill values are the same in the variograms calculated in different directions in this study. This also shows that the surface has geometric anisotropy (Armstrong 1998). It can be seen that the major axis of the anisotropic ellipse is trended NE-SW (Figure 4a). Experimental variograms have been calculated in 4 directions, which are N-S, E-W, NE-SW, and NW-SE. The lag size is 100 m and the angle tolerance is 45°. The experimental variogram has been fitted by an “*exponential variogram*” model (Figure 4b) that represents the direction of maximum continuity 55° from the north. In the experimental variogram, the sill

value is 5392.6 m, the range is 1280.39 m, and the nugget value is 10 m.

Neighborhood estimation, which defines a circle (or ellipse) including the predicted values on unmeasured points, is used to restrict the data (Johnston *et al.* 2001). While interpolating each grid node, the search ellipse defines the neighborhood of points to consider. Outside the search ellipse, the data points are not taken into account (Fencík & Vajsáblová 2006). In most cases, the search ellipse range and direction coincides with the anisotropy range and direction. At the same time, to prevent the tendency of particular directions, this circle (or ellipse) is divided into sectors. In this study, for determining the search ellipse, the anisotropy range and direction are used automatically and the ellipse is divided into 4 sectors. The maximum number of samples chosen is 6 for neighborhood estimation.

Cross-validation is used to control all numbers of data points (5292 points) used in interpolation. The graphic and table obtained after the cross-validation analysis are shown in Figure 5 and Table 1, respectively.

For perfect prediction, the estimation errors should be symmetrically distributed, and linear regression of exact values on estimated values should be close to a 45° line (Saraç & Tercan 1996). The needed criteria for the best created DEM were given by Johnston *et al.* (2001):

- Standardized mean nearest to 0.
- Smallest root mean square (RMS) prediction error.
- Average standard error nearest to the RMS prediction error.
- Standardized RMS prediction error nearest to 1.

Both the predicted values are nearly the same as measured values and the prediction error values indicate the satisfactory result of the interpolation (Figure 5; Table 1).

5. Three-dimensional subsurface modeling of mineralizations

The study area covers 1.4 km² (1 × 1.4 km) and elevation ranges from 270 m to 520 m. The surface has been divided

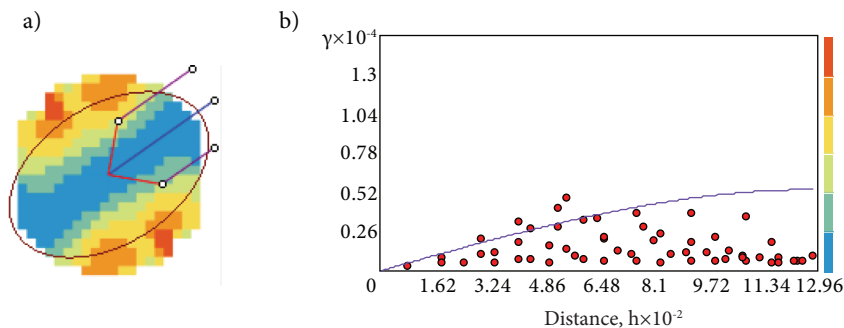


Figure 4. (a) Anisotropic ellipse showing NE-SW trend and the direction of the variogram, (b) experimental variogram in the direction of the major axis of the anisotropic ellipse.

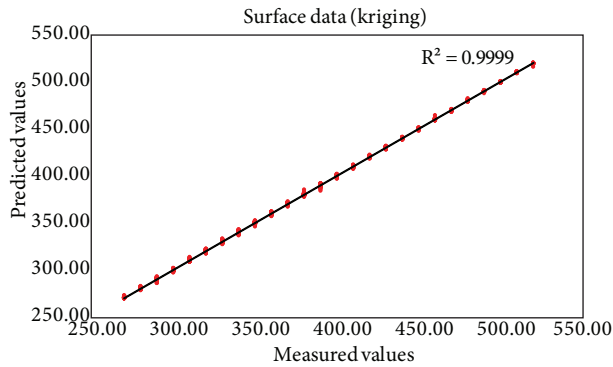


Figure 5. Cross-validation scatter plot of the surface data.

into $10 \times 10 \times 10$ m blocks (490,000 total voxels). In the northwestern and southeastern parts of the area, hilly topography with gentle slopes is seen while the Handeresi River flows from the northeast to southwest.

In order to create surface modeling, the topographic map (1/1000) of the study area (Yücelay 1976) is digitized, and x, y, and z values are entered into the *Geologic Utilities* section of RockWorks2006. Using these values, the software creates a grid-based file. While creating the grid file, the kriging method is used as an interpolation algorithm. One of the important features of RockWorks2006 software is that it is able to choose the most appropriate variogram that analyzes all the data automatically in the kriging interpolation method calculations. In this study, the “*Exponential with nugget*” variogram determined in accordance with the analysis of the software is preferred. Choosing the “*Exponential with nugget*” variogram automatically shows that the results in this analysis are also compatible with the results of geostatistical analysis. The 3D topographic surface modeling is intersected with a georeferenced geological map. Finally, the borehole point maps and the adits are done by drawing 3D borehole multilog (Figure 6).

The subsurface has been divided into $5 \times 5 \times 5$ m blocks. “ORE ZONE” applied to the *litho blend* algorithm and Pb%, Zn%, and Cu% values applied to *IDW* algorithm have 4,010,151 and 2,154,921 total voxel values, respectively.

Table 1. The summary statistics of the prediction errors using kriging interpolation with “*Exponential with nugget*” variogram.

Prediction errors	
Samples	5292
Mean	-0.007349
RMS	0.7163
Average standard error	1.6
Mean standardized	-0.0002796
RMS standardized	0.06106

In order to create subsurface modeling, 27 borehole data are taken from Yücelay (1976). The shallowest drilling is 60 m (S-01) and the deepest drilling is 245.65 m. (S-13). Total drilling depth is 4239.15 m while the average drilling depth is 157 m. The ore zones are observed in 6 out of 27 boreholes (S-04, S-06, S-14, S-15, S-19, and S-21). In order to determine Pb%, Zn%, and Cu% values in the ore zones, geochemical analysis was carried out according to the methods of Yücelay (1976). All of these values are entered into the RockWorks2006 software separately without any modification. The “ORE ZONE”, which is detected from drilling cores, is modeled via solid modeling. Here, while creating the block diagrams, the software makes the solid models of the lithologies using the *litho blend* algorithm (RockWare 2006). This algorithm is used to interpolate and extrapolate numeric values that represent “ORE ZONE” in the lithology class. Grid nodes between the boreholes are assigned a value that corresponds to the “ORE ZONE” section in the lithology class and relative proximity of each grid node to surrounding boreholes (Sweetkind *et al.* 2010). The model is intersected with topographic surface modeling. However, because of the insufficient number of drilled boreholes, the accuracy of the modeling of areas that are outside of the drilled area (Figure 7) is arguable.

Using the Pb%, Zn%, and Cu% geochemical analysis results, the model files are constructed separately using the *IDW* interpolation method. The parameters of the *IDW* interpolation method and 3D grade results are shown in Table 2 and Figure 8, respectively. The ore zones determined in the model files, due to the existence of ore zones in almost all boreholes, do not provide any focus area. One of the aims of this study is to lead to more detailed studies and to focus the ore zone(s) into more restricted areas. Determining of the area(s) in which Pb, Zn, and Cu mineralizations above the cut-off grades is thought to be ensured, as much as possible, close to the purpose described above. For this purpose, using Pb%, Zn%, and Cu% values with the above cut-off grades in all ore zones creates a database in RockWorks2006. In this software, this kind of subsurface data (such as those representing geochemistry, geotechnical measurements, etc.) is possible to model in 3D (*I-data* tool; RockWare 2006). Using this tool, RockWorks2006 interpolates the downhole interval-base data into a solid model. Solid modeling is implemented separately for the chemical analysis belonging to each element (Pb.mod file for Pb% modeling, Zn.mod file for Zn% modeling, and Cu.mod file for Cu% modeling; Figure 9a). As mentioned above, the ore zones that exist in almost all the boreholes reflect this modeling study, and large areas are detected for each element in the subsurface environment. Choosing a target area is difficult when the results are considered together. That is why using the intersections of all element zones

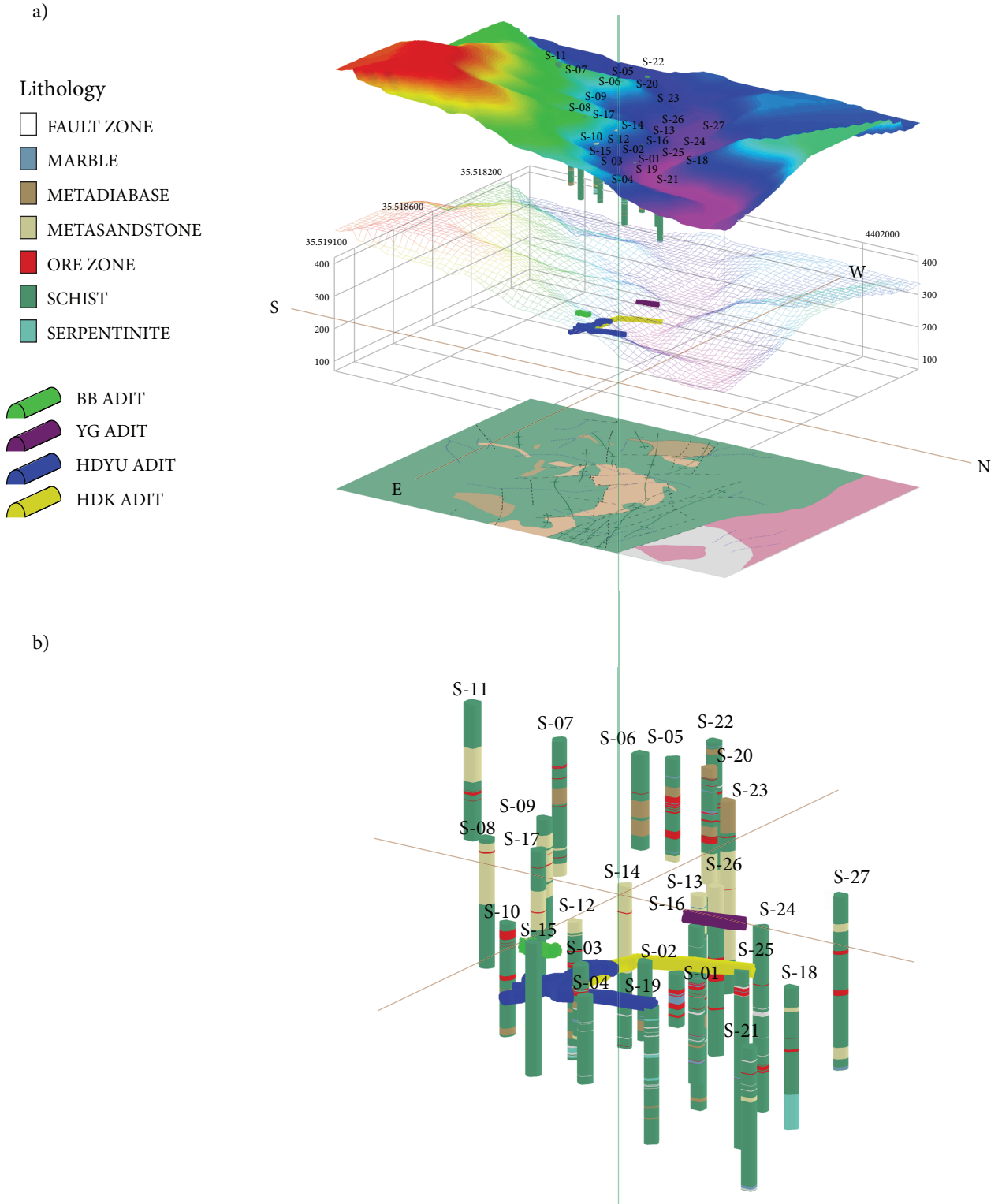


Figure 6. (a) 3D topographic surface modeling with borehole points, adits, and the geological map of the Handeresi area (to avoid confusion, -500 m offset is applied to the geological map (Figure 2) and +500 m offset is applied to the 3D topographic surface modeling along the z-axis). (b) 3D boreholes and adits of the Handeresi area.

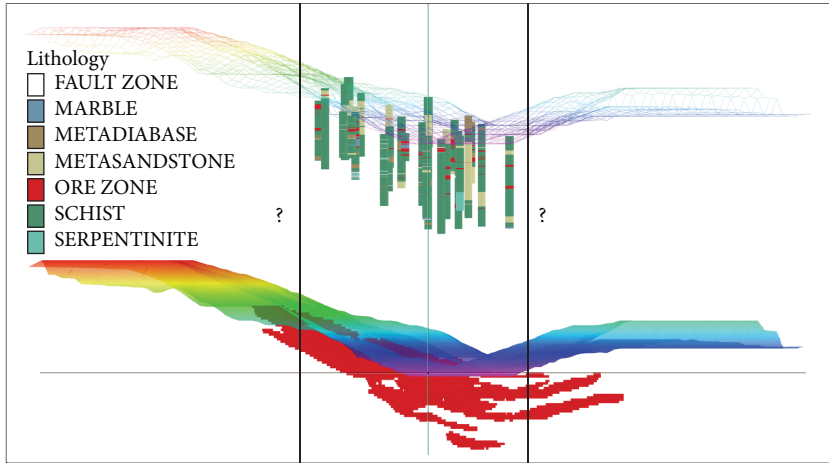


Figure 7. Topographic surface modeling, boreholes, and “ORE ZONE”, which is modeled with solid modeling of the Handeresi area (to avoid confusion, +500 m offset is applied to boreholes and upper surface modeling image along to z- axis); side of view: from NE.

(Pb%, Zn%, and Cu%) above the cut-off grades is more suitable for choosing a target area. If there are not enough boreholes without regular intervals, and if we do not detect the ore zones more precisely using these data separately, intersecting the areas above the cut-off grades gives the most promising fields. The probability of the presence of ores in these fields is the greatest. The purpose here is primarily to evolve model files in which the values above the cut-off grade get “1” and the values below the cut-off grade get “0”, and then to determine the “1” value in the file resulting from multiplying these model files with each other. In this latest model file, the areas having a “1” value indicate intersection of above the cut-off grade of Pb%, Zn%, and Cu%. In order to determine intersecting area(s) with the help of some arithmetic operations, new models need to be established. These operations are described below.

Rockworks Utilities includes several modeling tools, such as generating or making changes to a solid model. These are displayed under the *Solid* menu. The *Solid/Boolean Operations/Boolean Conversion* tool converts the real number solid model file to a Boolean (true/false)-type solid model file. In this process, the tool assigns a “1” if G-values of nodes fall within a user-defined range or assigns a “0” if they do not (RockWare 2006). In this study, the percentage value of the elements is assigned to

each solid model file as a G-value. The Pb% model file (Pb.mod) is chosen in the *Boolean Conversion* tool, and a value of “1” is assigned to 7% (Pb cut-off grade) and higher values. All values below 7% are accepted as “0” and a new model file consisting of Boolean values (Pb_boolean.mod) is created. All of these processes are applied separately to Zn% values with a 4% cut-off grade and Cu% values with a 0.3% cut-off grade, and Boolean model files are created (Zn_boolean.mod and Cu_boolean.mod, respectively).

For the next step, the *Solid/Math* tool, which includes the arithmetic operation, is applied to solid models. The

Table 2. The parameters of the *IDW* interpolation method.

Weighting exponent	4
Max. points per voxel	64
Max. points per borehole	32
Sector width	90°
Sector height	90°

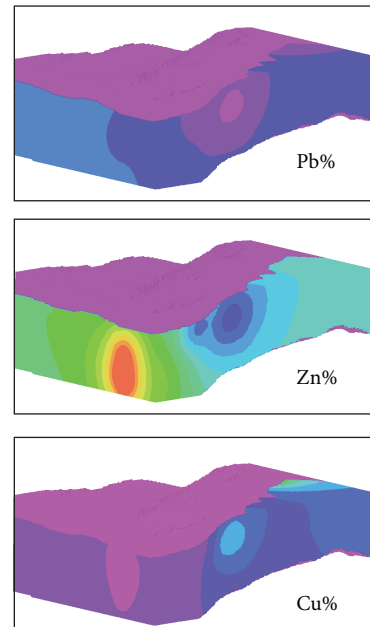


Figure 8. 3D grade model of the Pb%, Zn%, and Cu% distributions in the subsurface environment; side of view is the same in Figure 9. See Figure 11 for colored interval legends.

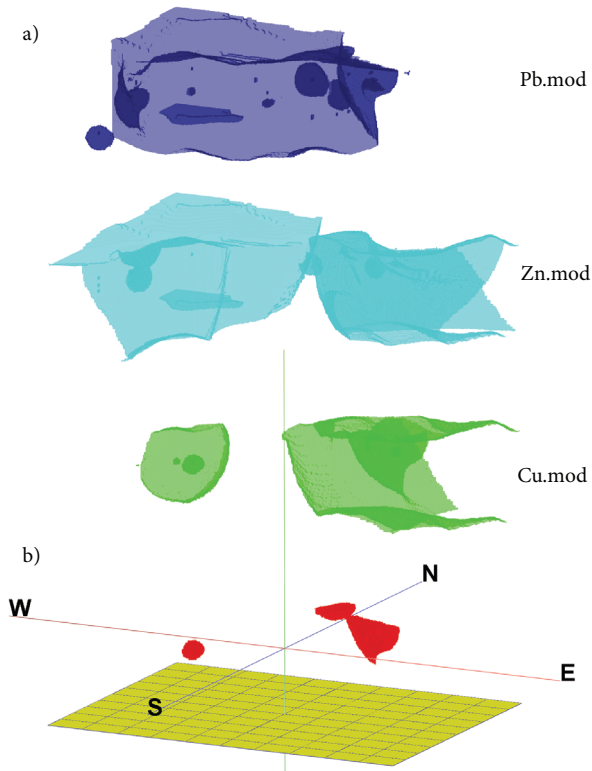


Figure 9. (a) The view of the “Pb.mod”, “Zn.mod”, and “Cu.mod” files after the solid modeling process is applied. (b) Visualization of the intersected zone after the Boolean-type solid modeling and mathematical operations are applied to “Pb.mod”, “Zn.mod”, and “Cu.mod” files.

options (*Model&Model*, *Model&Constant*, and *Resample*) within the *Solid/Math* tool are applied to arithmetic operations on the values in the solid model files previously created; this generates a new solid file (RockWare 2006).

The *Model&Model* tool applies arithmetic operations to the values of 2 model files and creates a new model file. In this study, the multiplication operation is applied to Pb_boolean.mod with Zn_boolean.mod files. As a result of the multiplication operation, the areas that include “1” values in both files (Pb and Zn cut-off grades and the higher values) indicate “1” values, while the other areas indicate “0” values in the newly created Boolean model file (Pb_Zn_boolean.mod). The multiplication operation is then applied for the generated file (Pb_Zn_boolean.mod) and the Cu_boolean.mod file. The created file (Pb_Zn_Cu_boolean.mod) at the end of this process includes “1” values that are assigned to Pb%, Zn%, and Cu% cut-off grades and higher values; the others include “0” values. The visualization of this modeling and schematic representations of these processes are shown in Figures 9b and 10, respectively.

In order to observe spatial distribution modeling in 2D, 2 cross-section lines (A-A’ and B-B’) are drawn containing the boreholes that take place in the possible ore zone areas (see Figure 2 for cross-section lines). In the first cross-section (A-A’), distribution of the ore zones is observed between and around S-01 and S-02 boreholes at elevations of about 225–300 m and around the S-17 borehole at elevations of 350–375 m. In the second cross-section (B-B’), distribution of the ore zones is observed around the S-23 borehole at elevations of about 215–240 m (Figures 11a and 11b). HDK and HDYU adits are situated near the S-01 and S-02 boreholes and the YG adit appears between the S-18 and S-01 boreholes in cross-section A-A’ (Figure 6). There are not any operating ore zone(s) and adits in the ore zones near the S-17 borehole in cross-section A-A’ or near the S-23 borehole in cross-section B-B’.

In the modeling study, it is important to correlate with measured values and predicted values, which are revealed

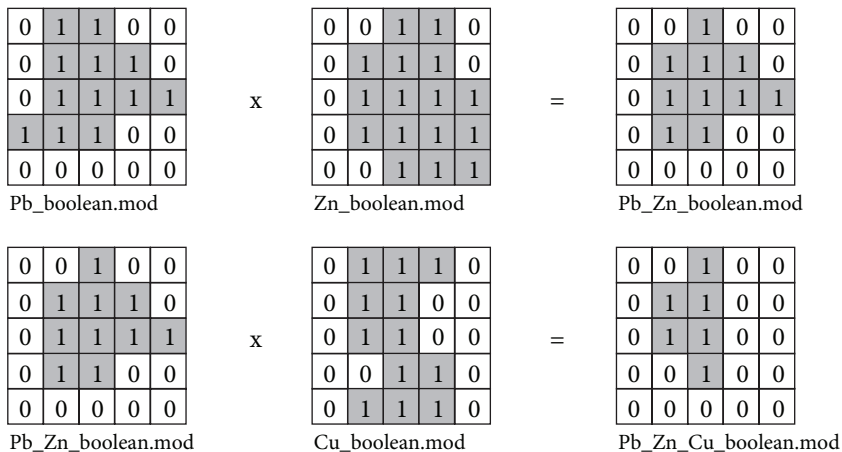


Figure 10. Schematic representations of the mathematical operations that are implemented to Boolean-type files. The “1” values indicate levels above the cut-off grades, while “0” values indicate levels below them (the values on these figures were arbitrarily selected).

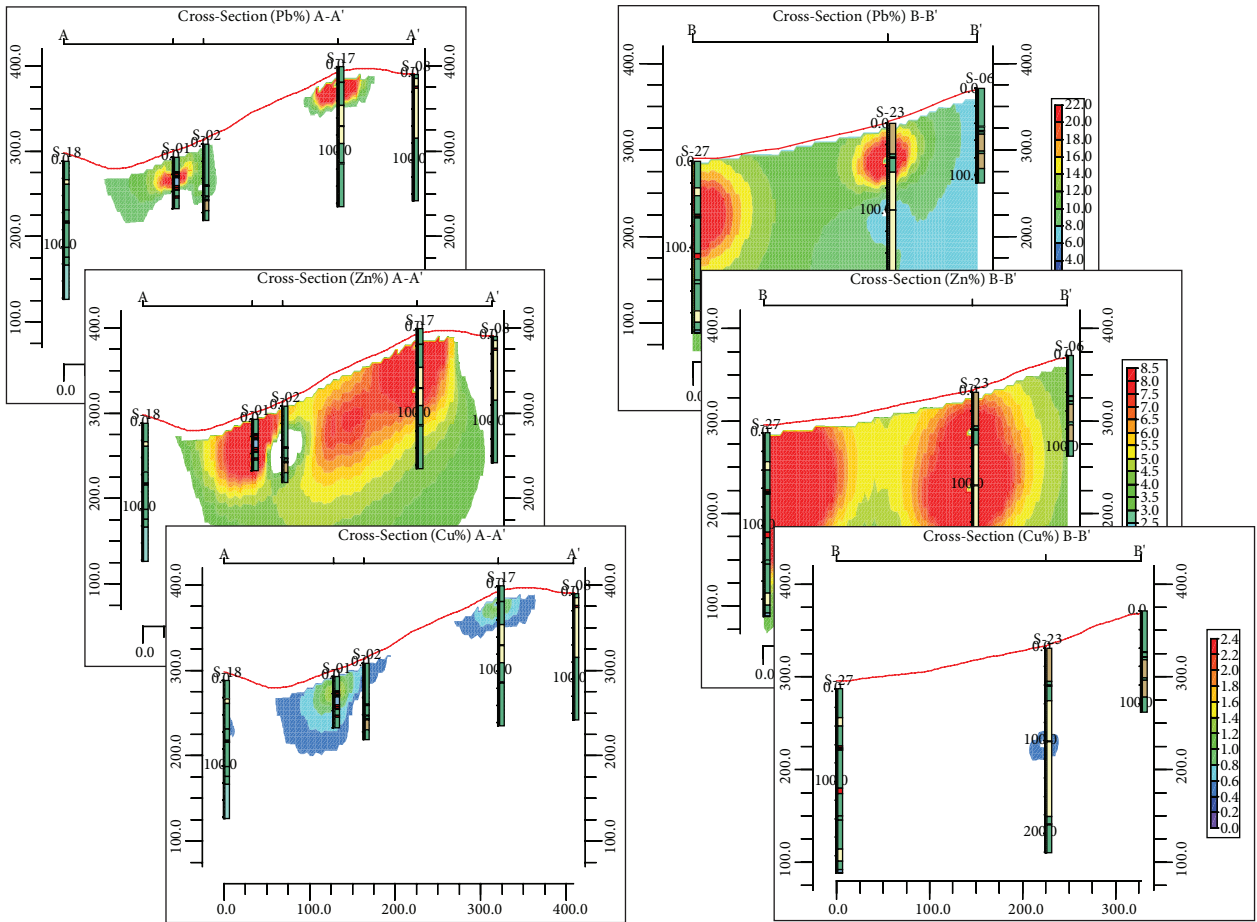


Figure 11. The cross-sections (a) (A-A') and (b) (B-B') of the Pb%, Zn%, and Cu% distributions at the subsurface (the red lines represent the topography). See Figure 2 for cross-section lines.

with the IDW interpolation method. The grid files are created using the arbitrarily selected 275-m elevation data (x, y coordinate values and g values) from the model files and then the created grid files are cross-validated using the Geostatistical Analyst Tool in ArcGis9 commercial software. Either the R^2 values are very close to the “1” value or the RMS values in the prediction errors get relatively low values, which indicates the accuracy of the interpolation method (Figure 12; Table 3).

6. Conclusions

With the help of computer technology, 3D subsurface modeling has been used quite frequently in the field of mineral exploration in recent years. The large amount of data obtained at regular spaces plays an important role in detecting the subsurface structures. In addition, reviewing previously collected insufficient data is very important in order to both clarify previously missed structures and focus on the work underway in specific areas. Furthermore, dense vegetation fields and/or high-slope areas make prospecting and geophysical studies

difficult. In these areas, to determine the potential areas on the surface and/or at the depths, the modeling study using borehole data is needed. Therefore, in this study, a target area that has irregularly spaced and insufficient boreholes, besides being explored actively at the present time and also covered with intensive vegetation, has been chosen. The use of active mining works is very important to compare the results.

As a result of the geostatistical analysis of the topographic data creating DEMs, the appropriate variogram type is determined and the results are checked mutually using the cross-validation procedures. Consequently, a DEM is created with the kriging interpolation method using the “Exponential with nugget” variogram.

In the Handeresi area, there are 27 boreholes that are intensively observed in 2 different areas; there are no other boreholes outside of these areas. For this reason, the complete subsurface modeling, using all lithologic variables, could not be implemented. Instead, the ore zones and Pb%, Zn%, and Cu% analytical results were modeled together. In addition, the faults in the area

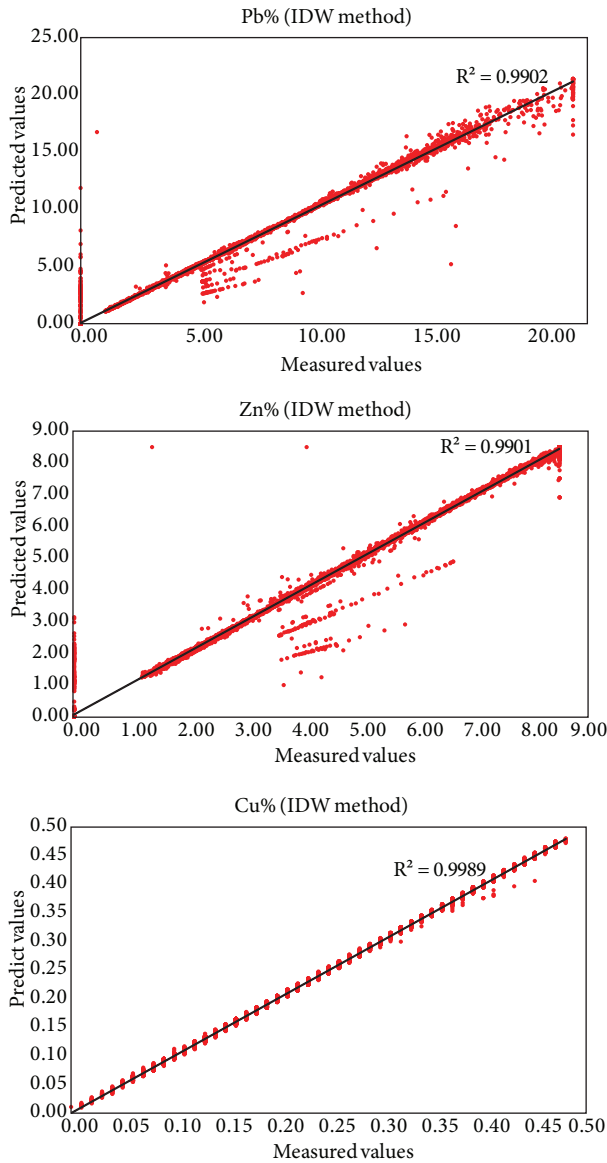


Figure 12. Cross-validation scatter plot of the geochemical analyses data.

are very important with respect to controlling the ore zones. Because the study area is covered with intensive vegetation, the direction of faults on the surface is detected with aerial photos (1/35,000 in scale) and a geologic map of the area drawn by Yücelay (1976). Because of many faults and the dividing of the study area into small blocks, the subsurface modeling and controlling the continuity of the mineralizations become complicated. Moreover, in the borehole determinations of Yücelay (1976), the exact measurements related to the fault zones could not be detected. That is the reason why the structural factors could not be reflected in the modeling study.

Some nearly accurate results have been obtained using the *IDW* interpolation method with the help of subsurface

Table 3. The summary statistics of the prediction errors using *IDW* interpolation methods.

	Prediction errors		
	Pb%	Zn%	Cu%
Samples	30,351	30,351	30,351
Mean	0.0000089	-0.0000166	0.0000011
RMS	0.3061	0.1581	0.003925

solid modeling, but due to inadequacies in the data, not enough detailed information could be obtained. As a result, there were 3 ore zones that were seen intensively in this area. One of them indicates the area in which the adits (Figure 6) are operating now (Zone 1, between and around S-01 and S-02 boreholes, Figure 11a). The other 2 represent the area that is still not in operation (Zone 2, S-17 borehole, Figure 11a; Zone 3, S-23 borehole, Figure 11b). In addition, the mineralization of Zone 1 is seen in the areas situated between 225 and 300 m elevations and near the HDK, HDYU, and YG adits. The mineralizations of Zone 2 and Zone 3 are observed at elevations of about 350–375 m and 215–240 m, respectively. In nearly of these zones, there are not any adits and/or mining operations. These zones could be new potential areas.

The zonal appearance of the ore mineralizations instead of along the specific zones is possible due to intensive faultings (Figures 11a and 11b). As mentioned above, the structural factors could not be reflected in the software program because of data deficiencies. However, due to the fact that the results are compared with the study area's data and the operated ore zones in the area are also detected in this study, the applicability of the modeling is brought out. In the future, during surface and subsurface exploration (e.g., boreholes, geophysical methods, well logs) in this area, using these data and focusing the studies on these zones will be much more economical with respect to the time and cost of mining operations. In addition, the data previously collected but lacking enough information to be evaluated can be used for determining potential new areas and/or developing areas being actively mined.

Acknowledgments

This work is a part of the PhD thesis of the first author at the Geological Department of Ankara University, supervised by the second author, and was also supported by the Scientific Research Office of Ankara University (BAPRO), Project No. 06B4343007. The authors wish to thank the 2 anonymous reviewers for their helpful reviews and also would like to thank Oreks Co. Ltd. for allowing access to the study area; Elif Akıska, Alper Gürbüz, and Kemal Mert Önal for sharing their important views; and Elaine Ambrose for revising the English in an early version of the manuscript.

References

- Akiska, S. 2010. *Yenice (Çanakkale) Bölgesi'ndeki Cu-Pb-Zn Oluşumları [Cu-Pb-Zn Occurrences of the Yenice (Çanakkale) Area]*. PhD thesis, Ankara University, Ankara, Turkey [unpublished].
- Akiska, S., Demirela, G., Sayılı, İ.S. & Kuşçu, İ. 2010a. Fluid inclusion and S isotope systematics of some carbonate-related Pb-Zn-Cu mineralizations in NW Anatolia, Turkey. *In: Melfos, V., Marchev, P., Lakova, I. & Chatzipetros, A. (eds), Geologica Balcanica Abstract Volume*, p. 21.
- Akiska, S., Sayılı, İ.S. & Demirela, G. 2010b. The subsurface 3D modeling of the Handeresi (Kalkim-Canakkale) area, NW of Turkey, Pb-Zn-Cu ore zones. *EGU2010 General Assembly, Vienna, Abstracts*, 1636.
- Armstrong, M. 1998. *Basic Linear Geostatistics*. Springer, Berlin.
- Binh, T.Q. & Thuy, N.T. 2008. Assessment of the influence of interpolation techniques on the accuracy of digital elevation model. *VNU Journal of Science, Earth Sciences* **24**, 176–183.
- Bistacchi, A., Massironi, M., Dal Piaz, G.V., Dal Piaz, G., Monopoli, B., Schiavo, A. & Toffolon, G. 2008. 3D fold and fault reconstruction with uncertainty model: an example from an Alpine tunnel case study. *Computers & Geosciences* **34**, 351–372.
- Brooker, P.I. 1986. A parametric study of robustness of kriging variance as a function of range and relative nugget effect for a spherical semivariogram. *Mathematical Geology* **18**, 477–488.
- Burrough, P.A. & McDonnell, R.A. 1998. *Principles of Geographical Information Systems*. Oxford University Press, Oxford.
- Çağatay, A. 1980. Batı Anadolu kurşun-çinko yataklarının jeoloji-mineraloji etüdü ve kökenleri hakkında görüşler [Geology and mineralogy of western Anatolian lead-zinc deposits and some comments about their genesis]. *Türkiye Jeoloji Kurumu Bülteni* **23**, 119–132 [in Turkish with English abstract].
- Çetinkaya, N., Karul, B., Önal, R. & Yenigün, K. 1983. *Geological Report on the Çanakkale-Yenice-Kalkım Handeresi Pb-Zn-Cu Mineralization*. General Directorate of Mineral Research and Exploration (MTA), Report No. 7822 [in Turkish, unpublished].
- Chaouai, N.E. & Fytas, K. 1991. A sensitivity analysis of search distance and number of samples in indicator kriging. *CIM Bulletin* **84**, 37–43.
- Chaplot, V., Darboux, F., Bourennane, H., Leguedois, S., Silvera, N. & Phachomphon, K. 2006. Accuracy of interpolation techniques for the derivation of digital elevation models in relation to landform types and data density. *Geomorphology* **77**, 126–141.
- Cressie, N.A.C. 1990. The origins of kriging. *Mathematical Geology* **22**, 239–252.
- de Kemp, E.A. 2000. 3-D visualization of structural field data: examples from the Archean Caopatina Formation, Abitibi greenstone belt, Québec, Canada. *Computers & Geosciences* **26**, 509–530.
- Demirela, G., Akiska, S., Sayılı, İ.S. & Kuşçu, İ. 2010. Silicate and sulfide mineral chemistry of some carbonate related Pb-Zn-Cu mineralizations and their effects on ore genesis in NW Anatolia, Turkey. *In: Melfos, V., Marchev, P., Lakova, I. & Chatzipetros, A. (eds), Geologica Balcanica Abstract Volume*, p. 91.
- Elkadi, A.S. & Huisman, M. 2002. 3D-GSIS geotechnical modeling of tunnel intersection in soft ground: the second Heineoord tunnel, Netherlands. *Tunnelling and Underground Space Technology* **17**, 363–369.
- Feltrin, L., McLellan, J.G. & Oliver, N.H.S. 2009. Modelling the giant, Zn-Pb-Ag century deposit, Queensland, Australia. *Computers & Geosciences* **35**, 108–133.
- Fencík, R. & Vajsáblóvá, M. 2006. Parameters of interpolation methods of creation of digital model of landscape. *The 9th AGILE Conference on Geographic Information Science*, Visegrad, Hungary, 374–381.
- Galera, C., Tennis, C., Moretti, I. & Mallet, J.L. 2003. Construction of coherent 3D geological blocks. *Computers & Geosciences* **29**, 971–984.
- Hack, R., Orlic, B., Özmutlu, S., Zhu, S. & Rengers, N. 2006. Three and more dimensional modelling in geo-engineering. *Bulletin of Engineering Geology and the Environment* **65**, 143–153.
- Harris, N.B.W., Kelly, S. & Okay, A.İ. 1994. Post collision magmatism and tectonics in northwest Anatolia. *Contributions to Mineralogy and Petrology* **117**, 214–252.
- Houlding, S.W. 1992. The application of new 3D computer modeling techniques to mining. *In: Turner, A.K. (ed), Three-Dimensional Modelling with Geoscientific Information Systems*. Kluwer Academic Publishers, Dordrecht, the Netherlands, 303–326.
- Houlding, S.W. 1994. *3D Geoscience Modeling: Computer Techniques for Geological Characterization*. Springer, Berlin.
- Johnston, K., Ver Hoef, J.M., Krivoruchko, K. & Lucas, N. 2001. *Using ArcGIS Geostatistical Analyst*. ESRI Press, Redlands, CA, USA.
- Kaufmann, O. & Martin, T. 2008. 3D geological modelling from boreholes, cross-sections and geological maps, application over former natural gas storages in coal mines. *Computers & Geosciences* **34**, 278–290.
- Krige, D.G. 1951. A statistical approach to some basic mine valuation problems on the Witwatersrand. *Journal of the Chemical, Metallurgical and Mining Society of South Africa* **52**, 119–139.
- Krushensky, R.D. 1976. Neogene calc-alkaline extrusive and intrusive rocks of the Karalar-Yeşiller area, Northwest Anatolia. *Bulletin Volcanologique* **39**, 336–360.
- Lam, N.S. 1983. Spatial interpolation methods review. *The American Cartographer* **10**, 129–149.
- Li, J. & Heap, A. 2008. *A Review of Spatial Interpolation Methods for Environmental Scientists*. Record 2008/23, Geoscience Australia, Canberra.
- Matheron, G. 1960. *Krigeage d'un Panneau Rectangulaire par sa Périphérie*. Note Geostatistique No. 28, CG. Ecole des Mines de Paris, Paris.
- Ming, J., Pan, M., Qu, H. & Ge, Z. 2010. GSIS: A 3D geological multi-body modeling system from netty cross-sections with topology. *Computers & Geosciences* **36**, 756–767.
- Okay, A.İ., Siyako, M. & Bürkan, K.A. 1990. Biga Yarımadası'nın jeolojisi ve tektonik evrimi [Geology and tectonic evolution of the Biga Peninsula]. *Türkiye Petrol Jeologları Derneği Bülteni* **2**, 83–121 [in Turkish with English abstract].

- Okay, A.İ., Satır, M., Maluski, H., Siyako, M., Monie, P., Metzger, R. & Akyüz S. 1996. Paleo- and Neo-Tethyan events in northwest Turkey: geological and geochronological constraints. In: Yin, A. & Harrison, M. (eds), *Tectonics of Asia*. Cambridge University Press, Cambridge, 420–441.
- Okay, A.İ., Satır, M. & Siebel, W. 2006. Pre-Alpide orogenic events in the Eastern Mediterranean region. In: Gee, D.G. & Stephenson, R.A. (eds), *European Lithosphere Dynamics*. Geological Society London, Memoirs **32**, 389–405.
- Özmutlu, S. & Hack, H.R.G.K. 1998. Excavatability evaluation and classification with knowledge based GIS. In: *Proceedings of 8th International IAEG Congress*, Vancouver, 591–598.
- Özmutlu, S. & Hack, R. 2003. 3D modelling system for ground engineering. In: Rosenbaum, M.S. & Turner, A.K. (eds), *New Paradigms in Subsurface Prediction Characterization of the Shallow Subsurface Implications for Urban Infrastructure and Environmental Assessment*, Lecture Notes in Earth Sciences, Vol. 99, Springer, Berlin, 253–260.
- Peralvo, M. 2004. Influence of DEM interpolation methods in drainage analysis. *GIS Hydro 04*, University of Texas, Austin, Texas.
- Rahman, K.M. 2007. *Settlement Prediction on the Basis of a 3D Subsurface Model, Case Study: Reeuwijk Area, the Netherlands*. MSc thesis, International Institute for Geo-Information Science and Earth Observation, Enschede, the Netherlands [unpublished].
- Renard, P. & Courrioux, G. 1994. Three-dimensional geometric modeling of a faulted domain: the Soultz Horst example (Alsace, France). *Computer & Geosciences* **20**, 1379–1390.
- Rengers, N., Hack, R., Huisman, M., Slob S. & Zigterman, W. 2002. Information technology applied to engineering geology. In: van Rooy, J.L. & Jermy, C.A. (eds), *Engineering Geology for Developing Countries - Proceedings of 9th Congress of the International Association for Engineering Geology and the Environment*, Durban, South Africa, 121–143.
- RockWare. 2006. *RockWorks® V.2006 - Earth Science and GIS Software*. RockWare, Golden, CO, USA. Available at http://www.rockware.com/assets/products/165/downloads/documentation/11/rw2006_manual.pdf [accessed 16 October 2011].
- Saraç, C. & Tercan, A.E. 1996. Grade and reserve estimation of the Tulovasi borate deposit by block kriging. *International Geology Review* **38**, 832–837.
- Sims, D.L. 1992. Application of 3D geoscientific modelling for hydrocarbon exploration. In: Turner, A.K. (ed), *Three-Dimensional Modelling with Geoscientific Information Systems*. Kluwer Academic Publishers, Dordrecht, the Netherlands, 285–290.
- Sweetkind, D.S., Taylor, E.M., McCabe, C.A., Langenheim, V.E. & McLaughlin, R.J. 2010. Three-dimensional geologic modeling of the Santa Rosa Plain, California. *Geosphere* **6**, 237–274.
- Tercan, A.E. 1996. Maden yatakları sınır belirsizliğinin indikatör kriging ile değerlendirilmesi ve Sivas-Kangal-Kalburçayırı kömür yatağında bir uygulama [Assessment of boundary uncertainty of ore deposits by indicator kriging and its application to the coal deposit of Kalburçayırı, Kangal, Sivas]. *Madencilik* **35**, 3–12 [in Turkish with English abstract].
- Tercan, A.E. & Saraç, C. 1998. *Maden yataklarının değerlendirilmesinde jeostatistiksel yöntemler [Geostatistical methods in the evaluation of ore deposits]*. TMMOB Jeoloji Mühendisleri Odası Yayınları **48**, Turkey [in Turkish].
- Tufan, A.E. 1993. *Karaydın Köyü (Yenice-Çanakkale) çevresinin jeolojik ve petrografik özellikleri ile kurşun-çinko zuhurlarının genetik incelemesi [Geological and Petrographical Characteristics of the Karaaydın Region (Yenice-Çanakkale) with the Genetic Investigations of Lead-Zinc]*. PhD thesis, Selçuk University, Turkey [in Turkish, unpublished].
- Turner, A.K. 1992. *Three-Dimensional Modelling with Geoscientific Information Systems*. Kluwer Academic Publishers, Dordrecht, the Netherlands.
- Veldkamp, J.G., Hack, H.R.G.K., Özmutlu, S., Hendriks, M.A.N., Kronieger, R. & Van Deen, J.K. 2001. Combination of 3D-GIS and FEM modelling of the 2nd Heineoord Tunnel, the Netherlands. In: *Proceedings of the International Symposium on Engineering Geological Problems of Urban Areas (EngGeolCity)*, Ekaterinburg, Russia, 1–8.
- Wang, G., Zhang, S., Yan, C., Song, Y., Sun, Y., Li, D. & Xu, F. 2011. Mineral potential targeting and resource assessment based on 3D geological modeling in Luanchuan region, China. *Computers & Geosciences* **37**, 1976–1988.
- Xue, Y., Sun, M. & Ma, A. 2004. On the reconstruction of three-dimensional complex geological objects using Delaunay triangulation. *Future Generation Computer Systems* **20**, 1227–1234.
- Yücelay, M.A. 1976. *The Etude of Çanakkale-Kalkım-Handeresi Pb-Zn-Cu Area*. General Directorate of Mineral Research and Exploration (MTA), Report No. 5720 [in Turkish, unpublished].
- Zanchi, A., Francesca, S., Stefano, Z., Simone, S. & Graziano, G. 2009. 3D reconstruction of complex geological bodies: examples from the Alps. *Computers & Geosciences* **35**, 49–69.
- Zhu, S., Hack, R., Turner, A.K. & Hale, M. 2003. How far will uncertainty of the subsurface limit the sustainability planning of the subsurface? In: *Proceedings of the Sustainable Development & Management of the Subsurface (SDMS) Conference*, Utrecht, the Netherlands, 203–210.
- Zimmerman, D., Pavlik, C., Ruggles, A. & Armstrong, P. 1999. An experimental comparison of ordinary and universal kriging and inverse distance weighting. *Mathematical Geology* **31**, 375–390.